Proceedings of ASME Turbo Expo 2003
Power for Land, Sea, and Air
June 16-19, 2003, Atlanta, Georgia, USA

GT2003-38083

DESIGN OF A MODERN TEST-FACILITY FOR LPT/OGV FLOWS

Johan Hjärne
Departement of Thermo and Fluid Dynamics
Chalmers University of Technology
412 96 Göteborg, Sweden
hjarne@tfd.chalmers.se

Jonas Larsson
Department of Aero and Thermo Dynamics
Volvo Aero Corporation
461 81 Trollhättan, Sweden
jonas.larsson@volvo.com

Lennart Löfdahl
Departement of Thermo and Fluid Dynamics
Chalmers University of Technology
412 96 Göteborg, Sweden
lelo@tfd.chalmers.se

ABSTRACT

This paper presents a complete design process of a modern test-facility for the investigation of low pressure turbine/outlet guide vane (LPT/OGV) flows. The design is based on modern CFD techniques combined with classical analytical approaches and experimental expertise. The paper describes the design procedure of the diffuser, the settling chamber, the contraction, the inlet section with boundary layer bleeds and the test-section. In the contraction part of the paper a new design method is developed using both separation and relaminarization theory. Finally, full viscous three-dimensional CFD calculations are performed of the test-facility, from the contraction to the test-section, making it possible to assess the flow characteristics of the test-facility before it is even constructed.

INTRODUCTION

Cost and weight requirements on modern jet engines often lead to more highly loaded turbines with fewer stages. In un-geared two and three shaft engines this gives higher swirl angles into the low pressure turbine/outlet guide vane (LPT/OGV) [1]. This, of course, makes the aerodynamic design of the OGVs more difficult. In addition, in recent LPT/OGV designs, structural requirements often lead to non-cylindrical shrouds with complex 3-dimensional polygonal shapes and sunken engine-mount bumps. This has sparked a renewed interest in design methods and validation cases for turbine OGV flows. A literature survey shows that very few, if any, measurements of realistic OGV flow-cases are publicly available.

The aerodynamic function of the LPT/OGVs is to turn the swirling flow out from the last low-pressure turbine rotor into an axial direction. This de-swirling gives a diffusive flow with growing boundary layers, strong secondary flows, and risk for separation both on vanes and end-walls. Non-cylindrical end-walls and engine mount bumps in the gas-channel further increases the risk of end-wall related separations and losses.

When designing an LPT/OGV the primary aerodynamic goal is to de-swirl the flow with as low total pressure losses as possible at the design point. In addition, to ensure that the engine works at all operating points, off-design requirements are often critical for the design. A typical LPT/OGV has inlet swirl angles up to around 25 degrees in the design point. In highly loaded turbines the swirl angle can be higher, sometimes as high as 45 degrees. At off-design points the swirl angle can vary +- 10 degrees from the design point.

To investigate on-design performance, off-design separations and end-wall bumps a blower linear cascade facility was chosen. This type of cascade makes it possible to carefully control the incoming boundary layers and cover a wide range of different inlet angles making the test-facility suitable for CFD validation. The test-facility will operate at atmospheric pressures and realistic Reynolds numbers, approximately 400000, implying velocities of just below 20m/s into the test-section with a chord-length of 200mm. This makes it possible to investigate the flow in detail, measuring pressure distributions, separations, wakes, outlet-angles and secondary flows. The Mach numbers are of course much lower than for a real engine and there will be no compressible effects. However,

Hjärne [2] confirmed with CFD simulations that compressibility effects are small for typical OGV flows.

A linear cascade will not be able to account for effects from rotor-vane interactions and a radial variation in the inlet condition. However, these phenomena can be covered with a CFD method validated with the data from the cascade. In Fig. 1 a bird's eye view of the test-facility is shown with the different parts which are described below.

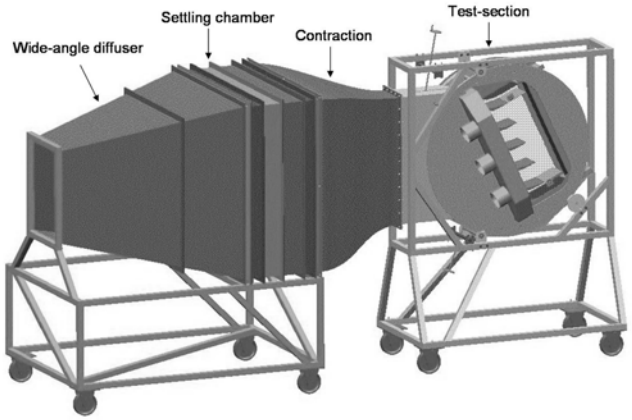

Figure 1. The test-facility

NOMENCLATURE

A	Area ratio between the diffuser outlet and inlet
AR	Aspect ratio of cross section area of the contraction
Cp	Pressure coefficient
CR	Contraction ratio
D	Square root of the contraction inlet area
H	Height of the contraction
K	Relaminarization parameter
L	Length
N	Number of screens
L/D	Relative length of the contraction
P	Pressure drop coefficient
R	Reynolds number
U	Local velocity
$\overline{U}$	Non-uniformity parameter
X	Location of the match point for the contours
W	Width of the contraction
n	Power factor of the polynomials
s	Contraction wall coordinate
x	x-coordinate

Greek Symbols

β	Open area ratio for screens
δ	Boundary-layer height
ν	Kinematic viscosity
σ	Standard deviation
θ	Half diffuser angle

Subscripts

lam	Laminar flow
max	Maximum
min	Minimum
mean	Mean value
r	Roof
turb	Turbulent flow
virtual	Virtual distance
w	Wall
1	Inlet
2	Outlet

1 WIDE-ANGLE DIFFUSER

Diffusers are used for converting velocity pressure into static pressure and for lowering the velocity coming from the blower. If the divergence of a diffuser is too rapid (the diffuser angle 2θ larger than 6 degrees) there exists a great risk of separation. Since separation of the flow in the diffuser leads to unsteadiness in the working section flow, separations most be avoided. However, a diffuser with a cone angle less than six degrees often gets too long which is undesirable both economically and because of unwanted growth of boundary-layers on the diffuser walls. So instead a shorter diffuser is designed and separation is avoided by the use of boundary-layer control which is the only way to avoid separation in a diffuser with a rapid cross-sectional area increase. Such a diffuser is called a wide-angle diffuser. As Mehta [3] states wide-angle diffusers is a means of reducing the length of a diffuser with a given area ratio, instead of something to effect pressure recovery.

Popular methods of boundary-layer control in wide-angle diffusers are insertion of screens, perforate plates or woven wire gauze. According to [3] screens make the velocity profile more uniform and reduces the boundary layer thickness leading to an increase in the ability to withstand separation. Mehta and Bradshaw [4] suggest that several screens of small pressure drop (P) are to be used instead of one with a large P, since increasing P at one position has little effect on the skin friction at a position further downstream.

There are four important parameters deciding the quality of the flow in a wide-angle diffuser, they are: area ratio (A), diffuser angle (2θ), pressure drop coefficient (P) and the number of screens within the diffuser (n). Mehta [3] collected data from over a hundred wide-angle diffuser designs and plotted design charts for the relevant parameters.

Following Mehta's [3] and Mehta and Bradshaw [4] design rules and suggestions a straight wall diffuser was created, see fig. 1 with characteristics according to table 1.

Table 1. Parameters for chosen diffuser

A	4,1
L (m)	1,5
2θ (°)	30
P	3
n	2

2 SETTLING CHAMBER

The settling chamber, located directly downstream of the wide-angle diffuser, is the section of the test-facility with the largest cross sectional area. The reason for this is that the flow conditioners situated here generates pressure drop. Therefore it is important that they are positioned in the part where the velocity is the lowest. This settling chamber will be equipped with one honeycomb and three screens.

A honeycomb is placed in the start of the settling chamber to straighten out the flow and suppress the incoming turbulence. It was shown by Loehrke and Nagib [5] that honeycombs both suppress the incoming level of turbulence, mostly due to the obstruction of the transverse velocity components from the cell side-walls, and generates new turbulence from shear-layer instabilities. The new turbulence, however, dissipates rapidly and this result in a net suppression of turbulence in the honeycomb. Since the generated turbulence is created from shear-layer instabilities it is of importance that the honeycomb is not too long, according to Burley and Harrington [6] Loehrke and Nagib [7] found that the length should not be grater than 12 times the honeycomb cell size.

Screens are used in wind-tunnel settling chambers to reduce free-stream turbulence and increase mean flow uniformity. Ability of suppressing turbulence increases with decreasing mesh size for a given screen open area ratio, β, consequently, subcritical screens greatly reduces turbulence. These screens however, tend to get clogged by dust particles and are not a good choice for settling chambers. Instead Groth and Johansson [8] suggest that several screens are to be used, even though this implies that the settling chamber will be longer. They also suggest that if screens are used in combination their separation should be chosen larger than the length of the initial decay region (the first 15-25 mesh widths) and to minimize the total pressure drop the other screens should be chosen with increasing mesh size in the upstream direction, i.e. the coarsest screen most upstream. Bradshaw [9] found that if β is less than 0.57 the screen may introduce flow non-uniformities. Therefore it was chosen to use screens with β above this level.

Some distance is needed behind a honeycomb or a screen for the turbulence to decay. According to Burley and Harrington [6] Loehrke and Nagib [7] have investigated this distance to be about 50 cell diameters, or 1 to 10 cell lengths for a honeycomb and for screens this distance is 50 to 75 mesh lengths or 330 to 500 wire diameters. If a screen is placed directly downstream of the honeycomb the distance for the turbulence to decay will be shorter. This was first shown by Loehrke and Nagib [5] and then investigated by Burley and Harrington [6]. The criterion deciding this distance is not dependent on honeycomb cell diameter and length but dependent on the ratio of honeycomb mesh to screen mesh, according to [6].

In the present settling chamber design, adjustment of the honeycomb/screen configuration is possible in order to be able to optimize the flow quality. As pointed out by Mehta and Bradshaw [4] it is important that the last screen is not to close to the contraction inlet otherwise distortion of the flow through the last screen may be expected.

3 CONTRACTION

One of the most important parts of the test facility is the contraction. Without a well designed contraction the flow quality into the test section will be poor. The purposes of the contraction is to; diminish flow disturbances coming from the settling chamber, accelerate the flow, keep the boundary layers down and create a uniform velocity profile going into the test section. The most important parameter determining the magnitude of these effects is the contraction ratio, CR. The challenge in contraction design is to find a contraction as small as possible without separation and with a good outlet flow quality.

When designing contractions of finite length, velocity extremes and adverse pressure gradients will appear near the ends, near the inlet a wall velocity minimum and near the outlet a wall velocity maximum, see Fig. 2. For three dimensional (rectangular) contractions, these maxima will appear in the corner regions of the contraction. The velocity extremes in the contraction lead to a non-uniform outlet velocity profile and risk of separation.

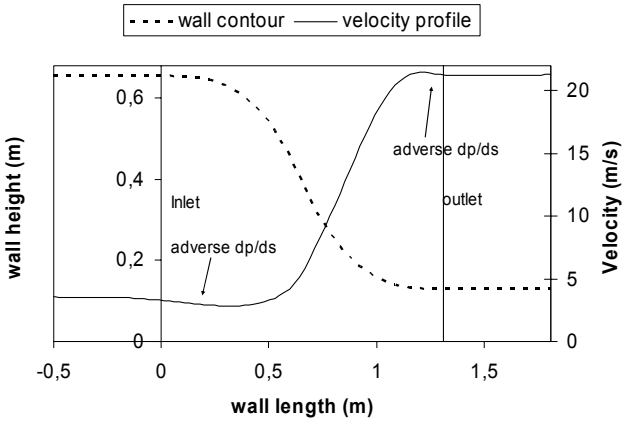

Figure 2. Velocity distribution on a contraction wall.

Three-dimensional contraction design has earlier been investigated numerically by [10-12]. The paper written by Fang [10] is focused on contractions with square end sections while the other two are more general and can be adopted for rectangular end sections as well. In the paper written by Su [11] a parametric study of important design parameters is conducted, based on criteria set up by Morel [13]. Here Su [11] states that three-dimensional contractions are worse than axisymmetric contractions when it comes to flow separation and exit flow non-uniformity. This is a result of the great velocity extremes produced in the corners of the contraction.

3.1 DESIGN CRITERIA

Key issues in contraction design are to prevent boundary-layer separation and to obtain a uniform outlet flow. Separations in the contraction can be devastating for the whole experimental setup. If the flow leaving the contraction has been exposed to separation, the flow quality will be poor, therefore it is of great importance to eliminate the risk of separation. There are different methods to investigate this, the most common method used in earlier works [10, 13, 14] is the one developed by Stratford [15]. This separation prediction method for turbulent boundary-layer flow results from an approximate solution of the equations of motion and is developed for flat plate boundary-layer theory. The equation states that separation will not occur as long as;

$$C_p\left(sdC_p/ds\right)^{\frac{1}{2}} - 0.35\left(10^{-6}R\right)^{\frac{1}{10}} < 0 \qquad (1)$$

where s is the coordinate following the wall, R is the Reynolds number and Cp is defined as;

$$Cp = 1 - \frac{U}{U_{\max}} \qquad (2)$$

This criterion is used for the adverse pressure region in the inlet part of the contraction since the flow coming from the settling chamber will be turbulent because of turbulence generation from tripping of the boundary-layers.

After the velocity minimum is reached the flow starts to accelerate strongly and relaminarization has to be investigated according to a criterion from the paper written by Back et al [16];

$$K = \frac{\nu}{U^2}\frac{dU}{ds} \tag{3}$$

Keeping in mind that relaminarization is a gradual and slow process it is not correct to associate it with a specific local value of K. Experiments by Back et al. [16] have though shown that when K exceeds a value of 2×10^{-6}, relaminarization effects will become important. After this relaminarization process has occurred it will not be correct to use Stratford's turbulent separation criterion any longer. Therefore it was chosen to use Stratford's laminar separation theory [15] after relaminarization occurred. Separation will not occur as long as;

$$C_p(s_{virtual}\frac{dC_p}{ds})^2 - 0.0076 < 0 \tag{4}$$

where $s_{virtual}$ is an equivalent length taken for a laminar boundary-layer to develop the correct height, obtained in the viscous computation described below, before the adverse pressure region appears. The laminar boundary-layer height is expressed as;

$$\delta_{lam} = 4.9\frac{s_{virtual}}{\sqrt{R}_{virtual}} \tag{5}$$

For a three-dimensional contraction like this there exists not only one *Cp*, as for axisymmetric contractions, but three; on the roof/floor, on the sidewalls and in the corners. In order to decrease the effect of the complex flow created in the corners, fillets will be inserted. When using fillets the Stratford criteria can be used, if the fillets are large enough to be approximated as a flat plate.

The second important design parameter mentioned above is the non-uniformity of the exit flow velocity. In several papers [10, 11, 13, 14] this parameter is expressed as Eq. (6);

$$\overline{U_2} = \frac{U_{2,\max} - U_{2,\min}}{U_{2,mean}} \tag{6}$$

Since this equation only accounts for peak values, it was decided to use the standard deviation according to Eq. (7) instead.

$$\sigma = \frac{\sqrt{\sum (U - U_{mean})^2}}{U_{mean}} \tag{7}$$

This criterion is a more stable way to decide if the whole flow field is uniform or not. For this test-facility it was decided that the standard deviation exiting the contraction not was allowed to reach 10%, and after the inlet channel it had to be less than 5%.

3.2 CONTRACTION GEOMETRY

The geometry chosen for this contraction consists of matched curves of the form;

$$C = \begin{cases} 1 - \dfrac{(x/L)^n}{X^{n-1}} & 0 \le \dfrac{x}{L} \le X \\ \dfrac{\left(1 - \dfrac{x}{L}\right)^n}{(1-X)^{n-1}} & X \le \dfrac{x}{L} \le 1 \end{cases} \tag{8}$$

where C stands for $(H-H_2)/(H_1-H_2)$ or $(W-W_2)/(W_1-W_2)$. These types of contours are the same investigated by [10, 11, 13, 14, 17]. From the paper written by Morel [13] it was concluded to use n=3, since this curve was analyzed to be the best for a short non-separating nozzle for axisymmetric designs. Without any further investigations it was assumed that these contours will be appropriate for a three-dimensional contraction as well.

When designing a contraction with these contours there are six parameters that define the geometry; the contraction ratio (CR), relative length (L/D), aspect ratio at entrance and exit (AR1, AR2), contour match points on the wall and the floor/roof (Xw and Xr). Based on the paper written by Su [11] it was decided that Xw=Xr=X and AR1=1 since the parametric study in this paper showed that these choices were the most favorable. AR2 was already decided since the pitch for the OGV:s was set and it was decided to use five OGV:s and two end-walls.

3.3 NUMERICAL INVESTIGATION

Both inviscid and viscous calculations have been performed for the investigation of the flow quality in the contraction. The commercial software code FLUENT [18] has been used for all the calculations. For the viscous calculations the Realizable k-ε turbulence model was used together with a two-layer zonal model for the near-wall flow.

For this test facility it was a wish to keep the contraction at a small size, both because of not risking to over contract the flow and to keep the boundary layers down as much as possible. Even though boundary-layer bleeds are going to be used on the side-walls the boundary layers will be held down to keep the bleeds thin. Other demands were, as mentioned earlier, that the standard deviation of the outlet flow uniformity not should be larger than 10% and of course no separation was allowed.

To find the optimum contraction for our needs it was chosen to investigate CR of 9, 7 and 6, L/D =0.85, 1 and 1.15 and X=0.4, 0.5, 0.55, 0.6, 0.7, 0.8, i.e. 54 different configurations altogether. From these investigations the final contraction was selected.

Inviscid calculations

With the inviscid calculations the separation risk using Stratford's criterions and the standard deviation of the outlet flow uniformity was investigated. Evaluating the results showed that the uniformity of the exit velocity decreased with higher CR and since this was one of the design criteria to be fulfilled it was in an early stage decided to use a CR as small as possible. It could also be seen that the exit conditions improved with increased length and was deteriorated with later match point, this is all shown in Fig. 4.

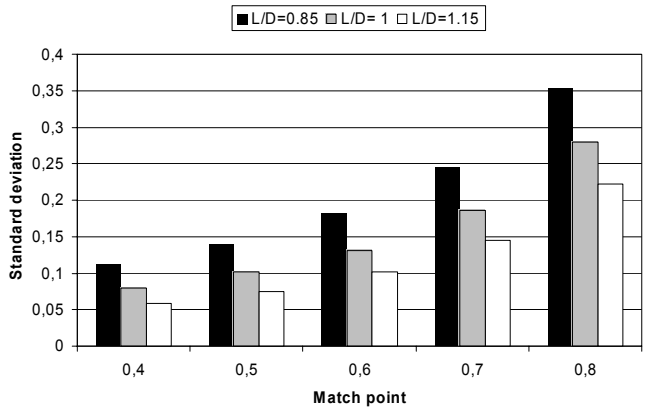

Figure 4. Standard deviation for outlet flow uniformity when CR=6 and L/D and X varies.

The other and maybe most important design criteria was whether or not the flow separated in the contraction. The most severe areas in terms of separation are the inlet and outlet corner regions where adverse pressure gradients exist. In Fig. 5 Eq. (1) is plotted for the inlet corner and in Fig. 6 Eq. (4) is plotted for the outlet corner. If the value on the y-axis exceeds zero there is a great risk of separation. In these figures it can clearly be seen that lengthening the contraction diminishes the risk for separation both on the inlet and on the outlet. In the outlet corner, Fig 6, the flow in all of the investigated contractions showed out to separate. The first thought to solve this problem is to lengthen the contraction, but from Eq. (5) $s_{virtual}$ was almost 80% longer than the actual s-coordinate of the contraction so making the contraction a little bit longer will not solve this problem. Instead this implies that the boundary-layer has to be tripped before the adverse pressure gradient arises in the outlet region, leading to a turbulent flow. When the boundary-layer turns turbulent the Stratford turbulent criterion can be used in the outlet region as well. Figure 7 shows that the risk of separation in the outlet corner has disappeared when making the boundary-layer turbulent.

One interesting observation made is that none of the contractions could withstand the process of relaminarization. This is because the velocity coming into the contraction is very low.

When deciding the position of matching of the two curves, it is a balance between, how good the inlet conditions will be compared to the outlet ones. If an early match point is chosen the inlet conditions may be a little worse compared to a later match point, and vice versa for the outlet. This implies that the best results are obtained for a match point of X around 0.5, which is why Fig. 5, 6 and 7 only shows the results with the match points X=0.5, 0.55 and 0.6.

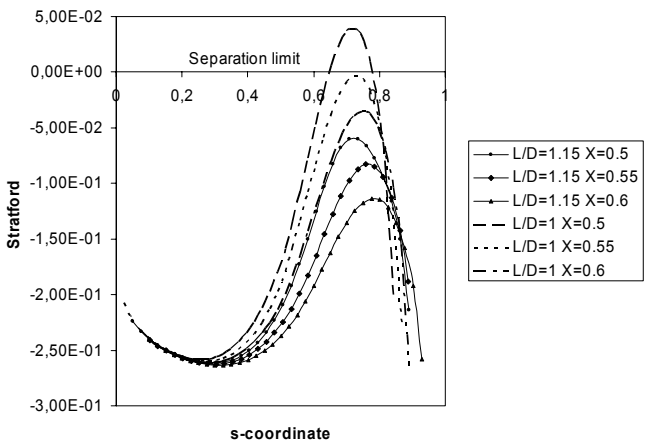

Figure 5. Eq. (1) for the inlet corner.

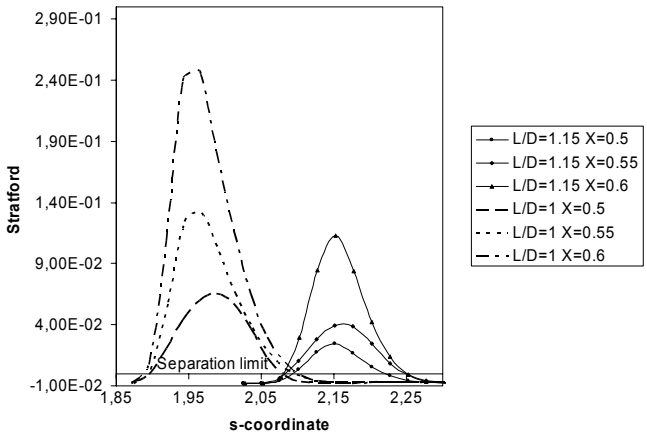

Figure 6. Eq. (4) for the outlet corner.

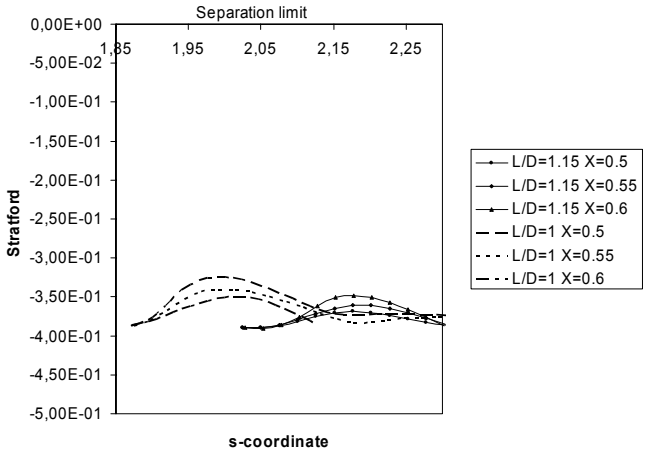

Figure 7. Eq. (1) for the outlet corner.

Viscous calculations

The viscous calculations were much more time-consuming so they have not been performed on all 54 combinations. Based on the results shown in Fig. 4, 5, 6 and 7 the following two configurations was chosen for detailed investigations, namely CR=6, L/D=1.15, X=0.5 and 0.55. In the viscous calculations it was of interest to evaluate the development of the boundary-layers in the contraction and

during the inlet to the test-section. Having a later match point maybe would suppress the boundary-layer significantly. Evaluating the results though showed that the difference in boundary-layer height was minimal and therefore the contraction with match point X=0.5 seemed to be the best for this test-facility. In Table 2 the parameters of the chosen contraction are listed and in Fig. 8 they are shown.

Table 2. Parameters for the chosen contraction.

CR	6
L/D	1.15
X	0.5
H1 (m)	1.31
H2 (m)	1.1
W1 (m)	1.31
W2 (m)	0.26

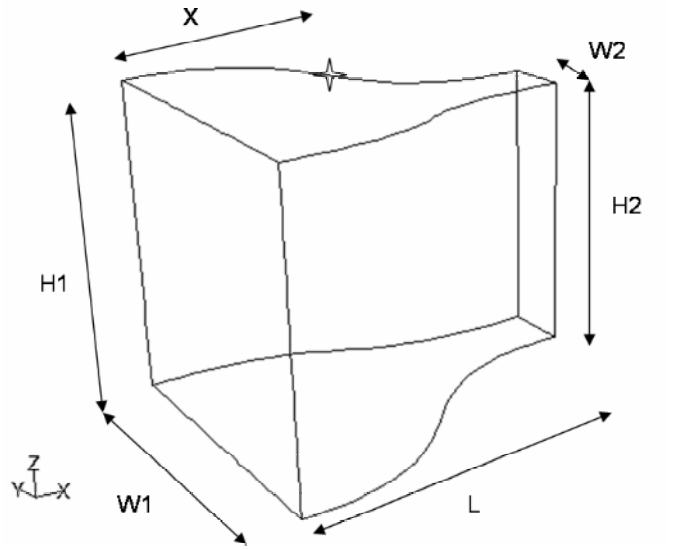

Figure 8. Dimensions of the contraction.

4 INLET AND TEST-SECTION

When the flow leaves the contraction it needs a certain distance before the non-uniformities are reduced below an acceptable level. With the use of the chosen contraction it was seen from viscous calculations that an appropriate inlet length should be 0.5 meters. At this distance the standard deviation of the outlet flow have been reduced from 7.5% to 3.8% which is in the limit of our demands.

The drawback with the inlet section is the boundary-layer development on the side walls. For real OGV flows the boundary-layers represent not more than 10% of the height of the OGV. To obtain similar boundary layer heights in the cascade the boundary-layers developed from the diffuser to the end of the inlet section have to be removed and rebuilt in the test-section. Therefore the cascade will be equipped with boundary-layer suction devices on the side-walls before the flow enters the test-section. Figure 9 shows that the boundary-layer bleed is located upstream of the OGVs and the space between the inner and outer disc serves as the suction slot. The distance between the cutting edge and the OGVs is 300mm. In this distance the boundary-layer height develops to 10 mm on the new side wall (or 5% of the width of the OGV) according to Eq. (10), which is the empirical evaluation of the development of turbulent boundary-layers,

$$\delta_{turb} = \frac{0.38x}{(R_x)^{0.2}} \qquad (10)$$

When cutting the boundary layer like this it is important that the streamlines diverges at the stagnation point of the cutting edge. To control if this is the case static pressure taps will be placed 10 edge diameters downstream of the edge on both sides of the plate. With these pressure taps it can be evaluated whether or not the static pressure is the same on both sides. The shape of the edge is also important; to start with an elliptic edge will be used since ellipsoids are known to be favorable in handling these kinds of flows. The boundary-layer height coming from the inlet side-walls is approximately 20mm, according to our calculations. To be on the conservative side it was chosen to make the slot 40mm wide. The suction system will be independent of the main air supply.

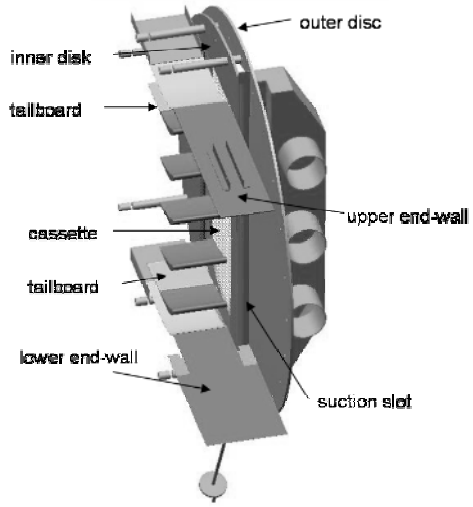

Figure 9. The test-section.

Another important property that has to be taken into account in LPT OGV flows is the free stream turbulence. The test-facility is designed both for the use of passive grids and active grids. To be able to vary the free-stream turbulence several slots will be prepared upstream of the test-section, were turbulence generating grids can be placed.

Following the inlet channel is the test-section. The test-section consists of two pairs of parallel discs where the inner discs constitute the side-walls of the five OGV's and the upper and lower end-walls. By turning the whole test-section, the inlet-angles can be varied continuously from 0 to 50 degrees, making it possible to cover both on- and off-design conditions. To make it easy to exchange vanes and end-walls, the vanes are mounted in a cassette. With this design it is possible to introduce contoured end-walls with engine-mount bumps or cassette walls of hard glass for the use of LDA (laser doppler anemometry).

A well defined periodicity of the flow around the OGV of interest is an essential requirement to achieve good measurement results; therefore great effort has been devoted on methods to control the periodicity. At first it was chosen to use six passages instead of only four since the periodicity around the mid OGV will increase with the number of passages. It was

also chosen to use end-walls which are adjustable with the turning of the test-section, i.e. as the test-section rotates the end-walls moves towards each other so the mass-flow into the test-section is controlled. It is also possible to change their outlet angle in the test-section. In addition to this two tailboards on OGV 1 and OGV 5 are mounted which are adjustable in any direction and can be used to tune the periodicity. Both the end-walls and the tailboards are adjustable during experiments, see Fig. 10.

By controlling the flow rate through the end passage slots, a strong effect on the variations in static pressure may be obtained and the setting may be optimized to give good upstream periodicity, according to [19].

Both upstream and downstream of the cascade there will be traversing systems. In the upstream traversing system, situated one chord upstream of the cascade, the inlet conditions will be measured, by means of pressure probes. With the downstream traversing system it will be possible to use both hotwires and pressure probes. The traversing system will be able to move in all directions and it will also be possible to tilt it to get into corner regions.

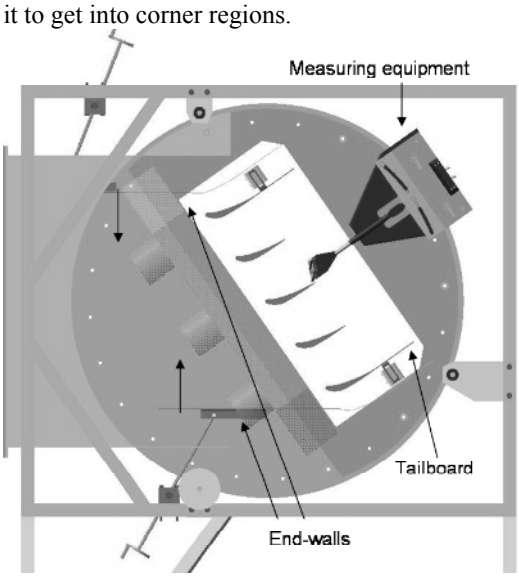

Figure 10. The test-section turned 30 degrees.

5 CFD CALCULATIONS OF THE TEST-FACILITY

To evaluate the quality of the test-facility before even building it, numerical simulations of the facility from the contraction to the outlet of the test-section have been conducted. Three-dimensional CAD geometries from CATIA were transformed and used in FLUENT [18]. On the final domain shown in fig. 11 full viscous three dimensional calculations were performed using a second order upwind scheme with the Realizable k-ε turbulence model and non-equilibrium wall functions. The aim with the calculations was to verify if any major mistakes had been done in the design of the test-facility and to evaluate certain parts and areas that were known to be hard to handle, such as the boundary-layer suction and periodicity.

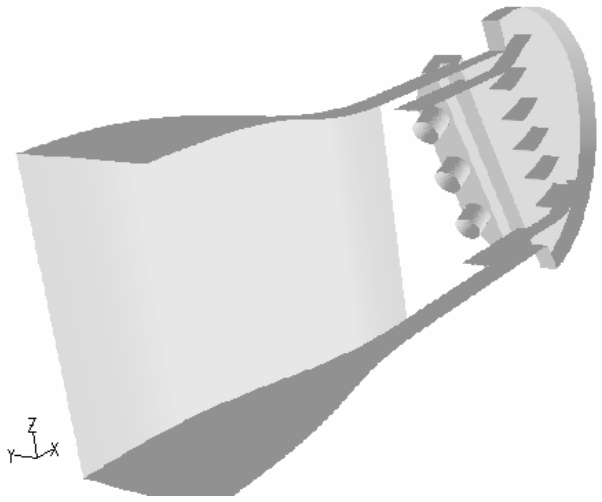

Figure 11. Computational domain with the inlet wall removed to make the boundary-layer suction device visible.

Cutting of boundary-layers is a sensitive process and some kind of control on how it is working has to be applied. As has been mentioned earlier static pressure taps will be placed along both sides of the cutting edge, to evaluate if the suction works properly and increase or decrease the rate of suction as necessary.

The first set of calculations were conducted without any vacuum added to the suction holes, for the simple reason that it was of interest to see if the air just could be raked off without any suction applied. To a certain extent this worked, but the obvious conclusion from these results was that the bleed caused a strong blockage effect on the flow which in turn affected the flow in the test-section. In fig. 12 the static pressure distribution is plotted in the symmetry plane of the inlet and the test-section. The blockage effect is clearly visible from the distinct pressure gradients just upstream of the cascade. The cause of the blockage effect is shown in fig. 13, visualizing that the velocity going into the suction chamber is higher in the upper parts of the bleed than the lower parts. When the high velocity flow hits the back wall of the suction chamber it deflects downwards and obstructs the flow in the lower parts of the bleed.

To prevent this blockage effect attempts by adjusting the suction rate through the three suction holes were made. At first an equal amount of vacuum was added to all holes. But when investigating the velocity profile into the suction bleed it was found that more fluid had to be sucked out of the lowest holes to even out the velocity profile, and get rid of the blockage effect. Although these changes improved the quality of the flow going into the test-section, they did not solve the problem entirely.

Next improvement was to insert a porous wall into the suction chamber to create a pressure drop and smooth out the velocity profile. This was a good method to even out the skewed velocity profile going both into the bleed and the test-section.

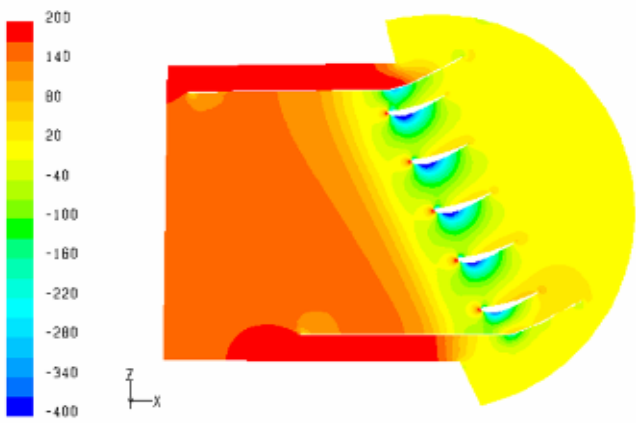

Figure 12. Static pressure distribution on the symmetry plane for the inlet and the test-section, when using no suction at all and only three suction holes.

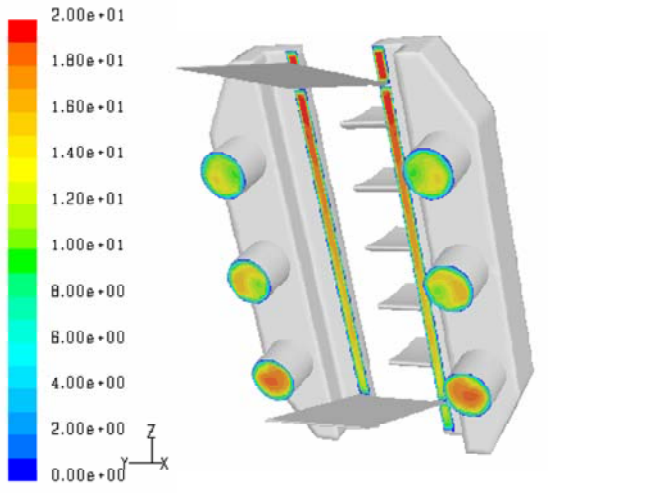

Figure 13. Velocity distribution for the suction slot and the outlet holes from the suction chamber.

Finally two more extra suction holes were added to improve the possibilities in controlling the suction, and to increase the area ratio between the bleed and the outlet suction. After doing all these changes and tuning the suction rate for the different holes the blockage effect was totally eliminated. Figure 14 show the new static pressure distribution after adding the porous wall and the two new holes. As can be seen the gradients are eliminated and we have approximately the same static pressure upstream of the whole cascade. What can be seen though is the strong effect from the end-walls disturbing the flow particularly in the lower passages.

In fig. 15 the velocity distribution of on an iso-plane taken at a constant z-coordinate is plotted to visualize the smooth velocity profile going into the test-section. This figure also shows the big difference in flow rate going out of the suction holes. To deal with this in the experimental setup it is planned to use perforated plates with adjustable porosity in front of the different holes.

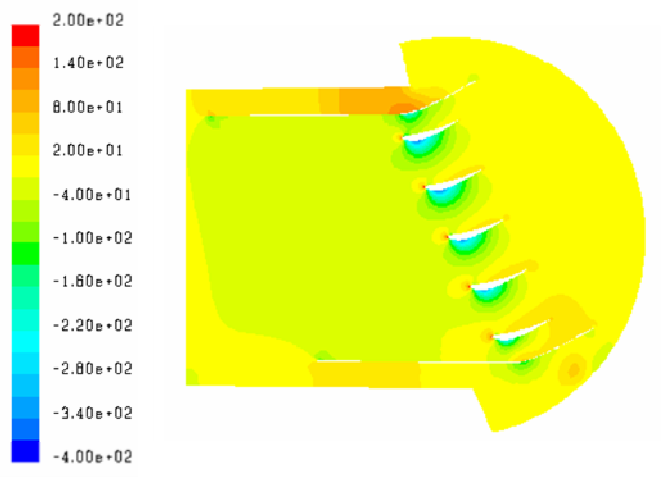

Figure 14. Static pressure distribution on the symmetry plane for the inlet channel and the test-section with the adjustments described in the text.

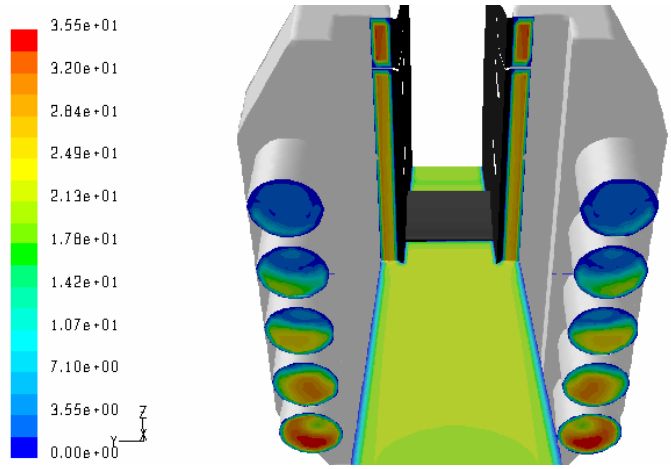

Figure 15. Velocity distribution going into the cascade taken at an iso-plane of constant z-coordinate.

When doing cascade experiments there always exist a risk of leakage flow, i.e. flow is sucked from the surroundings through leaks in the cascade. With the aid of CFD these areas can be located as for example in Fig. 14 it can be seen how negative pressure is distributed through out the inlet and the test-section giving information of where it is important to ensure that the test-facility is well sealed from the surrounding air.

Another interesting property to analyze is the periodicity. Figure 16 shows the static pressure distribution on the three mid vanes taken on the symmetry plane. In this figure it can clearly be seen that the pressure on the suction side of the three OGV's increases when approaching the lower passages. This is the result of the disturbance created by the end-walls. To prevent this in the experiment the end-walls have been designed to be both movable and lengthened during the experiment. Other methods to steer the periodicity is of course the use of tailboards, which are not included in these calculations, but will provide an extra tuning possibility of the periodicity.

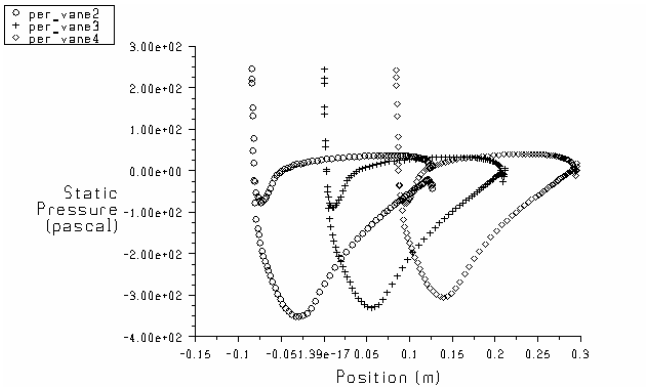

Figure 16. Static pressure distribution for the three mid vanes taken on the symmetry plane.

6 CONCLUSIONS

A complete design process of a low-speed linear cascade has been presented including design of settling chamber, contraction, boundary-layer suction device, test-section and periodicity-controlling possibilities.

In the contraction part of the paper a new design-method is presented using both turbulent and laminar separation theory together with relaminarization phenomenon. With this method a non-separating contraction with good outlet flow quality is developed.

The CFD analysis of the whole cascade is very valuable in the design process, providing the possibility to investigate the full flow field. Issues such as periodicity of the flow can easily be addressed and methods of how to improve the periodicity can be developed.

Another interesting phenomenon investigated was the boundary-layer suction system. The first calculations indicated a non-uniform velocity distribution in the suction slot, leading to a blockage of the flow field going into the test-section. With the aid of CFD we detected the problem and successfully developed different solutions and also possibilities to control and adjust this during experiments.

ACKNOWLEDGEMENTS

The present work is a part of the project COOL supported by the Swedish Gas Turbine Center, and funded by ALSTOM Power, Volvo Aero Corporation and Energimyndigheten. The permission for publication is gratefully acknowledged.

REFERENCES

[1] Vazquez, R., Cadrecha, D., Torre, D., and Morales, M., 2001, "Low Pressure Turbines with High Stage Loading," Proceedings of the ISOABE, Bangalore

[2] Hjärne, J., 2001, "Aerodynamic Analysis of Outlet Guide Vane Flows," Diploma thesis, Chalmers University of Technology, Göteborg, pp. 35-36

[3] Mehta, R. D., 1977, "The Aerodynamic Design of Blower Tunnels with Wide-Angle Diffusers," Prog. in Aerospace Science, **18**, pp. 59-120

[4] Mehta, R. D., and Bradshaw, P., 1979,"Design Rules for Small Low Speed Wind Tunnels, "The Aeronautical Journal, **83**, pp. 443-449

[5] Loehrke, R. I., and Nagib, H. M., 1976, "Control of Free-Stream Turbulence by Means of Honeycombs: A Balance Between Suppression and Generation," Journal of Fluids Engineering, pp. 342-353

[6] Burley, R. R., and Harrington, D. E., 1987, "Experimental Evaluation of Honeycomb/Screen Configurations and Short Contraction Section for NASA Lewis Research Center's Altitude Wind Tunnel," NASA Technical paper 2692

[7] Loehrke, R.I., and Nagib, H.M., 1972, "Experiments on Management of Free-Stream turbulence," AGARD R-598,

[8] Groth, J., and Johansson, A. V., 1988, "Turbulence Reduction by Screens," Journal of Fluid Mechanics, **197**, pp. 139-155

[9] Bradshaw, P., 1965, "The Effect of Wind Tunnel Screens on Nominally Two-Dimensional Boundary Layers," Journal of Fluid Mechanics, **22**, pp. 679-688

[10] Fang, Fuh-Min, 1997, "A Design Method for Contractions with Square End Sections," Journal of Fluids Engineering, **119**, pp. 454-458

[11] Su, Yao-Xi., 1991, "Flow Analysis and Design of Three-Dimensional Wind Tunnel Contractions," AIAA Journal, **29**, pp. 1912-1920

[12] Downie, J. H., Jordinsson, R., and Barnes, F. H., 1984, "On the Design of Three-Dimensional Wind Tunnel Contractions," Aeronautical journal, pp. 287-295

[13] Morel, T., 1975, "Comprehensive Design of Axisymmetric Wind Tunnel Contractions," ASME Journal of Fluids Engineering, pp. 225-233

[14] Morel, T., 1977, "Design of Two-Dimensional Wind Tunnel Contractions," ASME Journal of Fluids Engineering, pp. 371-378

[15] Stratford, B. S., 1958,"The Prediction of Separation of the Turbulent Boundary Layer," Journal of Fluid Mechanics, **5**, pp. 1-16

[16] Back, L. H., Cuffel, R. F., and Massier, P. F., 1968, "Laminarization of a Turbulent Boundary Layer in Nozzle Flow," AIAA Journal, **7**, pp. 730-732

[17] Callan, J. and Marusic, I., 2001, "Effects of Changing Aspect Ratio through a Wind-Tunnel Contraction," AIAA journal, **39,** pp. 1800-1803

[18] FLUENT 6, 2001, Users manual, Fluent Incorporated, Lebanon, NH, USA

[19] Gostelow, J.P., 1984, *Cascade Aerodynamics*, Pergamon, Oxford